Polyhedron 28 (2009) 3087–3093

Contents lists available at ScienceDirect

Polyhedron

journal homepage: www.elsevier.com/locate/poly

Synthesis, spectroscopic, thermal Studies, antimicrobial activities and crystal structures of Co(II), Ni(II), Cu(II) and Zn(II)-orotate complexes with 2-methylimidazole

Hakan Erer [a], Okan Zafer Yeşilel [a,*], Cihan Darcan [b], Orhan Büyükgüngör [c]

[a] Eskişehir Osmangazi University, Faculty of Arts and Sciences, Department of Chemistry, 26480 Eskişehir, Turkey
[b] Dumlupınar University, Faculty of Arts and Sciences, Department of Biology, 43010 Kütahya, Turkey
[c] Ondokuz Mayıs University, Faculty of Arts and Sciences, Department of Physics, 55139 Samsun, Turkey

ARTICLE INFO

Article history:
Received 5 May 2009
Accepted 19 June 2009
Available online 27 June 2009

Keywords:
Orotate complexes
2-Methylimidazole complexes
Antimicrobial activity

ABSTRACT

The 2-methylimidazole complexes of Co(II), Ni(II), Cu(II) and Zn(II) orotates, *mer*-[Co(HOr)$(H_2O)_2$(2-meim)$_2$] (**1**), *mer*-[Ni(HOr)$(H_2O)_2$(2-meim)$_2$] (**2**), [Cu(HOr)$(H_2O)_2$(2-meim)] (**3**) and [Zn(HOr)$(H_2O)_2$(2-meim)] (**4**), were synthesized and characterized by elemental analysis, spectral (UV–Vis and FT-IR) methods, thermal analysis (TG, DTG and DTA), magnetic susceptibility, antimicrobial activity studies and single crystal X-ray diffraction technique. The complexes **1** and **2** have distorted octahedral geometries with two monodentate 2-methylimidazole and one bidentate orotate and two aqua ligands. The complexes **3** and **4** have distorted square pyramidal and trigonal bipyramidal geometry, respectively, with one 2-methylimidazole, bidentate orotate and aqua ligands. The orotate coordinated to the metal(II) ions through deprotonated nitrogen atom of pyrimidine ring and oxygen atom of carboxylate group as a bidentate ligand. The antimicrobial activities of **1** and **4** were found to be more active gram (+) than gram (−) and **4** could be use for treatment *Staphylococcus aureus*.

1. Introduction

Supramolecular compounds have received much attention in coordination chemistry because of novel structural topologies and potential applications [1–3]. The non-covalent forces include hydrogen bonds and π···π interactions have been used extensively in the development of supramolecular chemistry. In the construction of new supramolecular complexes based the pyrimidine carboxylate ligands are of special interest, because they can be regarded not only as hydrogen bonding acceptors but also as hydrogen bonding donors, depending upon the number of deprotonated groups [4]. In the present work, we selected the potentially interesting orotic acid (1,2,3,6-tetrahydro-2,6-dioxo-4-pyrimidinecarboxylic acid, vitamin B13, H_3Or) that is a member of pyrimidine carboxylates. It is a useful tool for constructing crystalline architectures because of its proton donating and accepting capabilities for hydrogen bonds and π···π interactions [4,5].

Metal orotates are also widely applied in medicine and they have been used e.g. as uricosurica (for enhanced excretion of uric acid) and for electrolyte substitution (in heart and liver protection) [6]. Platinum, palladium and nickel orotates with wide variety of substituents have been screened as therapeutic agents for cancer [7–12].

Besides its important biological role, the mono- and dianion of orotic acid (H_2Or^- and HOr^{2-}) are potentially polydentate ligands. It may coordinate through two nitrogen atoms of the pyrimidine ring, two carbonyl oxygen atoms and carboxyl group [13–44]. It was found that, in neutral or slightly acidic environment, it coordinates through the carboxylate group [25–27] while in basic surroundings it coordinates through the carboxylate and the adjacent nitrogen atom [17]. In the *mer*-[Mn(μ-HOr)(H_2O)(2-meim)$_2]_n$ [16], [Ni(HOr)$(H_2O)_3$], [M(HOr)bipy(H_2O)] (M = Mn(II), Co(II)) [17], [Co(HOr)(OH)$(H_2O)(NH_3)]_n$ and [Ni(HOr)(OH)$(H_2O)_2(NH_3)]_n$ complexes [28], the orotate anion acts as a bridging ligand between the metal ions forming one-dimensional polymeric chains, its coordination sites being the carboxylate and the nitrogen atom of pyrimidine ring and carbonyl oxygen atom. In the polymeric [Cu(HOr)$(H_2O)_2]_n$ [29] and [Cu(HOr)$(ba)_2]_n$ [30] complex, molecules form chains in a way that the carboxylate group acts as a bridge between metal ions and the orotato-group being tridentate.

Recently, we have reported the synthesis and structures of orotate complexes of K(I) [15], Mn(II) [5,16], Co(II) [18,19,31–33], Ni(II) [19,34–39], Cu(II) [18,38–43], Zn(II) [44] and Cd(II) [20,45] with different aromatic amines.

In the present paper, we describe the syntheses, spectroscopic (IR and UV–Vis), thermal studies (TG, DTG, DTA), antimicrobial

* Corresponding author. Tel.: +90 2222393750; fax: +90 2222393578.
E-mail address: yesilel@ogu.edu.tr (O.Z. Yeşilel).

0277-5387/$ - see front matter © 2009 Elsevier Ltd. All rights reserved.
doi:10.1016/j.poly.2009.06.052

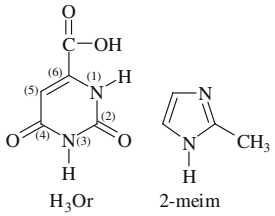

Scheme 1. Structures of the ligands: H_3Or = orotic acid; 2-meim = 2-methylimidazole.

activities and crystal structures of the orotate complexes of Co(II), Ni(II), Cu(II) and Zn(II) with 2-methylimidazole ligand (Scheme 1).

2. Experimental

2.1. Preparation of the complexes

A solution of orotic acid monohydrate (0.871 g, 5 mmol) in water (50 mL) was added dropwise with stirring at 80 °C to a solution of $Co(CH_3COO)_2{\cdot}4H_2O$ (1.25 g, 5 mmol) (**1**) or $Ni(CH_3COO)_2{\cdot}4H_2O$ (1.24 g, 5 mmol) (**2**) or $Cu(CH_3COO)_2{\cdot}H_2O$ (1.00 g, 5 mmol) (**3**) or $Zn(CH_3COO)_2{\cdot}2H_2O$ (1.09 g, 5 mmol) (**4**) in distilled water (25 mL). The solutions immediately became suspensions and were stirred for 4 h at 60 °C. Then 2-methylimidazole (1.65 g, 20 mmol) for all in water (10 mL) was added dropwise to these suspensions. The clear solutions that formed were stirred for 2 h at 60 °C and then cooled to room temperature. The reddish for (**1**), green for (**2**), light blue for (**3**), colorless for (**4**) crystals that formed were filtered and washed with 10 mL of water and dried in air.

2.2. Materials and measurements

All chemicals used were analytical reagents and were commercially purchased. IR spectra were obtained with a Perkin Elmer 100 FT-IR spectrometer using KBr pellets in the 4000–400 cm^{-1} range. The UV–Vis spectra were obtained for an aqueous solution of the complex (10^{-3} M) with a Shimadzu UV-3150 spectrometer in the range 900–190 nm. Magnetic susceptibility measurements at room temperature were performed using a Sherwood Scientific MXI model Gouy magnetic balance. A Perkin Elmer Diamond TG/DTA Thermal Analyzer was used to record simultaneous TG, DTG and DTA curves in static air atmosphere at a heating rate of 10 °C min^{-1} in the temperature range of 30–1000 °C for **1** and 30–700 °C for **2**–**4** using platinum crucibles.

2.3. Crystallographic analyses

Data collection was performed on a STOE IPDS II image plate detector using Mo Kα radiation (λ = 0.71073 Å). Data collections: Stoe X-AREA [46]. Cell refinement: Stoe X-AREA [46]. Data reduction: Stoe X-RED [46]. The structure was solved by direct-methods using SIR97 [47] and anisotropic displacement parameters were applied to non-hydrogen atoms in a full-matrix least-squares refinement based on F^2 using SHELXL-97 [48]. Molecular drawings were obtained using ORTEP-III [49].

2.4. Antimicrobial activity studies

Escherichia coli W3110, *Pseudomonas aeruginosa* ATCC 27853, *Staphylococcus aureus* ATCC 6535, *Bacillus cereus* ATCC 7064, *Candida albicans* ATCC 10231 and clinical isolate (Methicillin Resistant *S. aureus* (MRSA) – Orthopedy Exuda, *Pseudomonas aeruginosa* – urology–urine isolates, from Ondokuz Mayıs University, Faculty of Medicine) were used for the antimicrobial assays. Antimicrobial activity tests were carried out using the broth dilution method as described by the NCCSL standards [50]. All stock solutions of the orotic acid and the complexes were prepared in dimethylsulfoxide (DMSO, Merck) according to the needed concentrations for experiments.

For the broth dilution method, cultures were grown in 5 mL nutrient broth (Merck) at 37 °C for 18 h in an orbital shaker incubator shaking at 175 rpm. These cultures were used as starter cultures. Initial bacterial concentrations (approximately 5×10^5 cfu/mL) were estimated for the cultures at 600 nm by matching with 0.5 McFarland turbidity standards. Nutrient broth containing microorganisms were transferred 1 mL in test tubes and made twofold serial dilution in nutrient broth from 3000 to 23.4 μg/mL. The compounds were tested in twofold serial dilution; eventually the ranges were narrowed to define more exact values. Growth inhibition was determined by measuring MICs, defined as the lowest concentration in which microbial growth was prevented. As indicated by the lack of turbidity or colour change after 24 h of incubation at 37 °C, represents the mean of at least three determinations. The solvents were also tested for antimicrobial activity. Standard antibiotics (chloramphenicol, oflaxacin, rifampicin, cefuroxime, tetracycline, nystatin) were also tested by disc diffusion method for the cultures at an optical density at 600 nm by matching with 0.5 McFarland turbidity standards (approximately 10^6 cfu/mL). Test strains were spread on solid nutrient agar surfaces using a sterile glass rod. Standard antibiotic discs were placed on the agar surface and were incubated 37 °C for 24 h.

3. Results and discussion

The Co(II), Ni(II) and Cu(II) complexes exhibit magnetic moment values of 4.66, 2.54 and 1.26 BM which corresponds to three, two and one unpaired electrons, respectively, which are consistent with a weak field octahedral geometry as expected. The Zn(II) complex is diamagnetic. All the complexes comprise broad composite bands in the UV region, being due to $\pi \rightarrow \pi^*$ and $n \rightarrow \pi^*$ intraligand transitions of HOr and 2-meim ligands. The λ_{max} value of the absorption band in the spectrum of **1** is 499 nm. This value was assigned to the following d–d transitions, $^4T_{1g} \rightarrow {}^4T_{2g}$. The $^4T_1g \rightarrow {}^4A_{2g}$ and $^4T_{1g} \rightarrow {}^4T_{1g}(P)$ transitions were not observed which are shift to the UV and IR regions, respectively. The UV–Vis spectrum for **2** exhibits three d–d absorption transitions at 888, 638 and 390 nm which support the octahedral geometry. These values were assigned to $^3A_{2g} \rightarrow {}^3T_{2g}$, $^3A_{2g} \rightarrow {}^3T_{1g}$, $^3A_{2g} \rightarrow {}^3T_{1g}$ (P), respectively. The UV–Vis spectrum for **3** exhibits a broad d–d absorption transition centered at 707 nm. This value was assigned to a1 → b1 transition. The colourless Zn(II) complex does not show d–d bands as expected.

The strong and broad absorption bands of ν(OH) vibrations of H_2O in complexes are observed between 3402 and 3361 cm^{-1}. IR spectra of the complexes exhibit a medium intensity and broad band in the 3272–3178 cm^{-1} region which can be attributed to the N–H stretching vibration. The relatively weak two close bands at 2752–2964 cm^{-1} are due to the ν(CH) vibrations. The strong and broad bands appeared in the 1653–1623 and 1488–1382 cm^{-1} regions in all complexes are ascribed to the asymmetric and symmetric stretching vibrations of the coordinated carboxylate groups of the orotate ligand, respectively. Similar absorption values have already been reported earlier for Ni(II) and Co(II)-orotate complexes with imidazole and its derivatives [16,19,33,51] and the positions of these bands have been well described in recently reports [52]. Separation between asymmetric and symmetric stretching frequencies for complexes range from 167 to 141 cm^{-1} is in agreement with monodentate coordination mode for the

Table 1
IR data of the complexes.[a]

Assignment[a]	Co(II)[b]	1	2	3	4
ν(OH)	3544s	3402s, br	3361s, br	3400s	–
νNH_{meim}	3255m	3266m	3268m	3272m	3254sh
νNH_{HOr}	3207m	–	3199sh	3204w	3178br
νCH	3087–2971w	3092sh–2925m	3104sh–2930m	3120sh, 2925w	2930w
$\nu C{=}O_{acid} + \nu C_{(2)}{=}O$	1639s	1642s	1651s	1653s	1651s, br
$\nu C_{(6)}{=}O + \nu C{=}C$	1620s	1623s	1628s	1626s	1628s
$\nu C{=}N$	1483m	1486m	1488s	1485m	1484m
δNH	1427w; 1373m	1398m, 1382m	1399s, 1382m	1399vs	1392s
M–O; M–N	522w; 466w	595w, 481m	576m, 487m	593m	583m, 481m

[a] *Abbreviations*: sh, shoulder; w, weak; m, medium; s, strong; vs, very strong; br, broad.
[b] $[Co(HOr)(H_2O)(4\text{-meim})_3]$ [19].

carboxylate group. In IR spectra of the complexes, $\nu(OH_{acid})$ band at 2500 cm^{-1} in the orotic acid completely disappeared and a new carboxylate band ν(COO) appeared between 1488 and 1382 cm^{-1}, respectively, indicating that the carboxylate group participates in the coordination with the metal ions by deprotonation (Table 1).

3.1. Thermal analyses

3.1.1. $[Co(HOr)(H_2O)_2(2\text{-meim})_2]$ (**1**) and $[Zn(HOr)(H_2O)_2(2\text{-meim})]$ (**4**)

The thermal behaviour of **1** and **4** are quite similar and they show a three stage mass loss (Supplementary Figs. S1 and S2). The first stage between 37 and 199 °C for **1**, 33 and 212 °C for **4** corresponds to the endothermic elimination of two aqua ligands with an experimental mass loss of 9.06% and 11.19% (calc. mass loss 8.71% and 10.66%). The removal of 2-meim ligands occurs in the second stage between 199 and 391 °C for **1**, 212 and 373 °C for **4** with an experimental mass loss of 40.54% and 23.49% respectively (calc. mass loss 39.73% and 24.32%). In the last stage, a strong exothermic peak on the DTA curve (DTA_{max} = 423 and 529 °C, respectively) is associated with decomposition and burning of the orotate ligands. The overall experimental mass losses, 82.92% for **1** and 75.18% for **4**, are in agreement with this stoichiometry. The thermal decomposition products were identified as CoO or ZnO (calc. 81.85% and 75.88%).

3.1.2. $[Ni(HOr)(H_2O)_2(2\text{-meim})_2]$ (**2**)

The complex **2** shows three stages decomposition process (Supplementary Fig. S3). Although the complex is containing aqua ligands, it is stable up to 151 °C. In the first stage, complex **2** starts to lose aqua ligands between 151 and 225 °C with an experimental mass loss of 8.71% (calc. mass loss 9.73%). The second stage is related to the release of two imidazole ligands by giving endothermic effect (found = 41.11, calc. = 39.74%). This type of behaviour of methylimidazole ligands in the *mer*-$[Mn(\mu\text{-}HOr)(H_2O)(2\text{-meim})_2]_n$ [16] and $[Ni(HOr)(H_2O)(4\text{-meim})_3]$ [19] complexes have been reported earlier. In the last extremely exothermic stage between 398 and 474 °C orotate ligand is abruptly burnt (DTA = 454 °C). The total mass loss of all decomposition process is 82.82% (calc. 81.88%) suggest that NiO is the end product.

3.1.3. $[Cu(HOr)(H_2O)_2(2\text{-meim})]$ (**3**)

The complex **3** shows four stages decomposition process (Supplementary Fig. S4). In the first stage, the complex starts to lose one aqua ligand between 37 and 160 °C with an experimental mass loss of 5.65% (calc. 5.36%). The second stage is related to the release of other aqua ligand by giving endothermic effect (found = 6.22, calc. = 5.36 %). The third stage in the temperature range of 246–288 °C related to release of 2-meim ligand (found 23.42, calc. 24.45%, DTA_{max} = 267 °C). In the last extremely exothermic stage between 288 and 458 °C orotate ligand is abruptly burnt (DTA = 423 °C). The total mass loss of all decomposition process is 77.61% (calc. 76.29%) suggest that CuO is the end product.

3.2. Crystal structures

Details of crystal data, data collection, structure solution and refinement are given in Table 2. The molecular structures of **1** and **2** with the atom-numbering scheme are shown in Fig. 1. Selected bond lengths and angles together with the hydrogen bonding geometry are collected in Table 3. The structures of **1** and **2** consist of the *mer*-$[M(HOr)_2(H_2O)_2(2\text{-meim})_2]$ (M = Co(II) and Ni(II)) molecules. Both metal ions are coordinated bidentate orotate ligand thought oxygen atom of carboxylate group and nitrogen atom of pyrimidine ring, two aqua ligands and two 2-methylimidazole ligands. The basal plane of the distorted octahedral is formed by N1, O4, O5 and O6 atoms. The Co–O (average 2.108 (1) Å), Ni–O (average 2.071 (1) Å) and Co–N1 (2.138 (1) Å), Ni–N1 (2.087 (1) Å) bond distances are longer than previously reported values ($[Co(HOr)(H_2O)_4]\cdot 2.5H_2O$ [47], $[Co(HOr)(en)_2](H_2Or)\cdot 5H_2O$ [18] and *mer*-$[Ni(HOr)(H_2O)_2(ata)_2]$ [43]). However these bond distances are similar to the corresponding values found in reported $[Co(HOr)(H_2O)_3]_n$, $[Ni(HOr)(H_2O)_3]_n$ [23] and [Ni(HOr)(bipy)] [53]. Distorted octahedral geometry is completed with two nitrogen atoms by monodentate coordination of two 2-meim ligands (Co1–N3/N5 = 2.164(2)/2.158(2) and Ni1–N3/N5 = 2.127 (2)/2.123 (2) Å).

The crystal packing of **1** and **2** are stabilized through strong intra- and intermolecular hydrogen bonding interactions (Fig. 2a). Each HOr ligand is doubly hydrogen bonded forming DA:AD dimer between the O1, N2 of HOr and the O4 atom of carboxylate group and aqua ligand (O5) [N2···O4 = 2.896 (2) for **1**, 2.882 (2) for **2** and O5···O1 = 2.757 (2) for **1**, 2.736 (2) for **2**] with a pattern $R_2^2(8)$ in Etter's notation [54]. There are also $\pi\cdots\pi$ interaction between the symmetry related 2-meim rings [Cg*A* = N(3)–C(6)–C(7)–N(4)–C(8) and Cg*B* = N(5)–C(10)–C(11)–N(6)–C(12), Cg*A*–CgA^i = 3.8251 (i = $-x$, $-y$, $-z$) and Cg*B*–CgB^i = 3.9814 Å, i = $1-x$, $1-y$, $-z$) (Fig. 2b).

In pentacoordinated systems, the actual geometry of the complex can be described by a structural index parameter τ such that $\tau = \alpha - \beta/60°$, where α and β are the two largest angles ($\alpha > \beta$). Thus, the geometric parameter τ is applicable to pentacoordinated structures as an index of the degree of trigonality, within the structural continuum between trigonal bipyramidal (τ = 1) and square pyramidal (τ = 0). The complex **3** and **4** have τ values of 0.20 for **3** [$\tau = (169.81 - 158.00)/60 = 0.20$] and 0.60 for **4** [$\tau = (164.91 - 128.77)/60 = 0.60$], indicating a distorted square bipyramidal and trigonal bipyramidal geometries, respectively (Fig. 3). The M ion in $[M(HOr)(H_2O)_2(2\text{-meim})]$ (M = Cu(II) and Zn(II)) is coordinated by a bidentate HOr ligand, two coordinated water molecules and one 2-meim ligand [Cu1–N1 = 1.992(2), Cu1–O4 = 2.073(1), Zn1–O4 = 2.083 (2) and Zn1–N1 = 2.066 (2) Å]

Table 2
Crystallographic data and structure refinement parameters for the complexes.

Complexes	**1**	**2**	**3**	**4**
Empirical formula	$C_{13}H_{18}N_6O_6Co$	$C_{13}H_{18}N_6O_6Ni$	$C_9H_{12}N_4O_6Cu$	$C_9H_{12}N_4O_6Zn$
Formula weight	413.26	413.04	335.77	337.60
Crystal system	monoclinic	monoclinic	triclinic	triclinic
Space group	$P2_1/c$	$P2_1/c$	$P\bar{1}$	$P\bar{1}$
a (Å)	8.3165 (4)	8.2609 (5)	7.5760 (6)	7.1751 (5)
b (Å)	14.1580 (4)	14.1719 (6)	8.1422 (6)	8.2451 (6)
c (Å)	15.3992 (7)	15.3190 (9)	11.5213 (9)	11.9655 (8)
α (°)	90	90	69.657 (6)	73.759 (6)
β (°)	102.478 (4)	102.791 (5)	85.372 (6)	87.218 (6)
γ (°)	90	90	77.057 (6)	71.923 (5)
V (Å^3)	1770.35 (13)	1748.93 (17)	649.43 (9)	645.51 (8)
Z	4	4	2	2
μ (mm^{-1})	1.01	1.15	1.71	1.94
D_{calc} (Mg m^{-3})	1.551	1.569	1.717	1.737
Crystal size (mm)	0.35 × 0.30 × 0.23	0.58 × 0.49 × 0.41	0.46 × 0.33 × 0.25	0.37 × 0.28 × 0.14
θ Range (°)	1.98–26.5	1.98–26.5	1.89–26.5	2.71–26.5
Measured reflections	14 984	13 938	7124	6765
Independent reflections	3679	3633	2677	2668
R_{int}	0.025	0.041	0.046	0.047
$R[F^2 > 2\sigma(F^2)]$, $wR(F^2)$	0.028, 0.079	0.028, 0.080	0.030, 0.079	0.034, 0.091
Goodness-of-fit on F^2	1.04	1.07	1.09	1.05
$\Delta\rho_{max}$, $\Delta\rho_{min}$ (e Å^{-3})	0.27; −0.40	0.29; −0.30	0.57; −0.56	0.45; −0.62

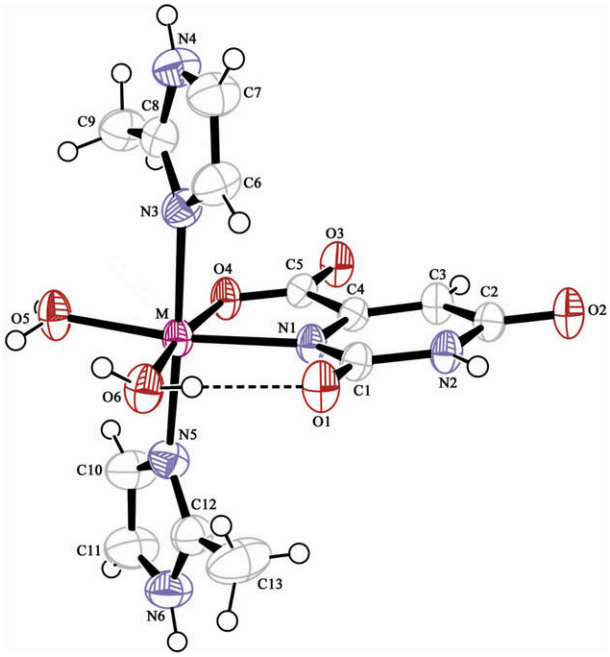

Fig. 1. Ortep III view of **1** and **2** with the atom-numbering scheme (M = Co1 and Ni1).

(Table 4). These distances are found to be similar to those of previously reported complexes [7,18,41,55]. The dihedral angle between the pyrimidine and imidazole rings is 67.65 Å for **3** and 66.79 for **4**. The C5–O4 bond distance (1.260 Å for **3** and 1.251 Å for **4**) is longer than C5–O3 bond distance (1.240 Å for **3** and 1.241 Å for **4**) in HOr ligand due to the coordination of M(II) ion.

The presence of aqua ligands and carboxyl or carbonyl groups make extensive hydrogen bonding interactions in complexes **3** and **4**, which are listed in Table 4. Each of the HOr ligand is doubly hydrogen bonded to corresponding ligands of a neighbouring HOr ligand, forming DA:AD dimer [N2···O2^{i} = 2.830 (**2**) for **3** and 2.897 (**3**) Å for **4**, N2–H2···O2^{i} = 172 for **3** and 170° for **4**, (i) $-x+2$, $-y$, $z+1$ for **3** and $x+2$, $-y$, $-z+1$ for **4**]. These arrangement gives rise

Table 3
Selected bond distances (Å), angles (°) and hydrogen bonding geometries (Å, °) for **1** and **2**.

Bond lengths (Å)			
Complex **1**		Complex **2**	
N1–Co1	2.138 (1)	N1–Ni1	2.0874 (13)
N3–Co1	2.164 (2)	N3–Ni1	2.1272 (15)
N5–Co1	2.158 (2)	N5–Ni1	2.1233 (15)
O4–Co1	2.104 (1)	O4–Ni1	2.062 (1)
Co1–O5	2.105 (1)	Ni1–O5	2.070 (1)
Co1–O6	2.114 (1)	Ni1–O6	2.081 (1)
Angles (°)			
O4–Co1–O5	92.42 (5)	O4–Ni1–O5	91.95 (5)
O4–Co1–O6	171.52 (5)	O4–Ni1–O6	173.61 (5)
O5–Co1–O6	95.83 (5)	O5–Ni1–O6	93.98 (5)
O4–Co1–N1	79.18 (5)	O4–Ni1–N1	80.55 (5)
O5–Co1–N1	170.23 (5)	O5–Ni1–N1	171.01 (5)
O6–Co1–N1	92.76 (5)	O6–Ni1–N1	93.74 (5)
O4–Co1–N5	87.98 (5)	O4–Ni1–N5	88.09 (5)
O5–Co1–N5	88.50 (6)	O5–Ni1–N5	88.86 (6)
O6–Co1–N5	90.28 (6)	O6–Ni1–N5	89.65 (6)
N1–Co1–N5	96.11 (6)	N1–Ni1–N5	95.79 (5)
O4–Co1–N3	90.88 (5)	O4–Ni1–N3	90.98 (5)
O5–Co1–N3	88.54 (6)	O5–Ni1–N3	88.24 (6)
O6–Co1–N3	91.28 (6)	O6–Ni1–N3	91.59 (6)
N1–Co1–N3	86.63 (5)	N1–Ni1–N3	86.95 (5)
N5–Co1–N3	176.78 (6)	N5–Ni1–N3	176.92 (5)
D–H···A	H···*A* (Å)	*D*···*A* (Å)	*D*–H···*A* (°)
*Complex **1***			
N2–H2···O4^{i}	2.04	2.8960 (18)	177
N6–H6C···O2^{ii}	2.10	2.906 (2)	156
N4–H4···O3^{iii}	2.03	2.843 (2)	157
O6–H6B···O1	1.939 (16)	2.7373 (19)	156 (2)
O5–H5B···O2^{iv}	1.858 (17)	2.6689 (18)	166 (2)
O5–H5A···O1^{v}	1.899 (16)	2.7572 (19)	175 (2)
O6–H6A···O3^{vi}	1.888 (17)	2.7065 (18)	169 (2)
*Complex **2***			
N2–H2···O4^{i}	2.02	2.8818 (19)	177
N6–H6C···O2^{ii}	2.09	2.900 (2)	156
N4–H4···O3^{iii}	2.02	2.830 (2)	156
O6–H6B···O1	1.938 (16)	2.7358 (18)	155 (2)
O5–H5B···O2^{iv}	1.851 (17)	2.6661 (18)	166 (2)
O5–H5A···O1^{v}	1.935 (16)	2.7730 (19)	176 (2)
O6–H6A···O3^{vi}	1.906 (18)	2.7150 (17)	165 (2)

Symmetry codes: (i) x, $-y+1/2$, $z+1/2$; (ii) $-x+1$, $y-1/2$, $-z+3/2$; (iii) $-x+1$, $-y+1$, $-z+1$; (iv) $x-1$, $-y+1/2$, $z-1/2$; (v) x, $-y+1/2$, $z-1/2$; (vi) $x-1$, y, z for **1** and **2**.

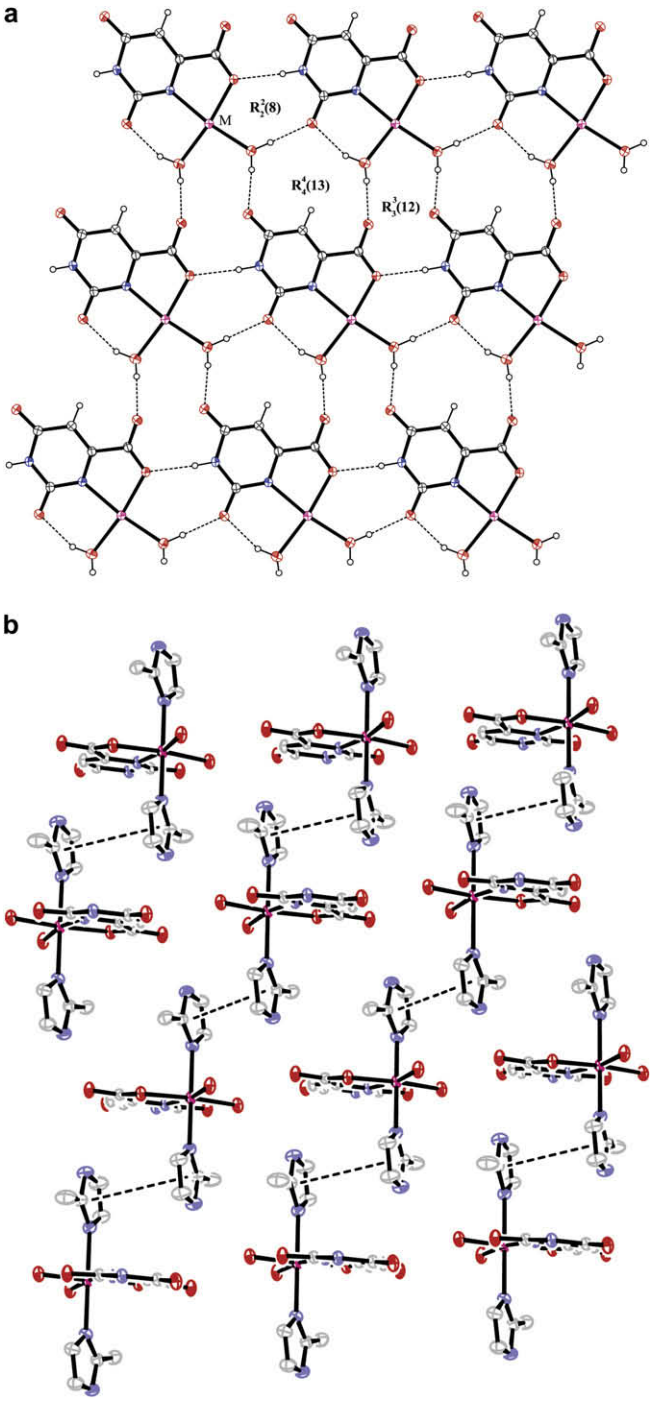

Fig. 2. Part of the crystal structure of **1** and **2**, showing the formation of hydrogen bonding [2-meim ligands are omitted] (a) and π···π interaction [H atoms are omitted] (b).

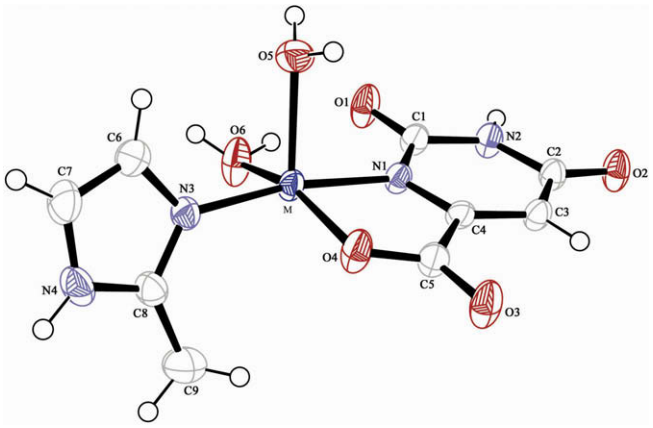

Fig. 3. Ortep III view of **3** and **4** with the atom-numbering scheme (M = Cu1 and Zn1).

Table 4
Selected bond distances (Å), angles (°) and hydrogen bonding geometries (Å, °) for **3** and **4**.

Bond lengths (Å)			
Complex **3**		Complex **4**	
N1–Cu1	1.992 (2)	N1–Zn1	2.066 (2)
N3–Cu1	1.961 (2)	N3–Zn1	2.008 (3)
O4–Cu1	1.973 (2)	O4–Zn1	2.083 (2)
Cu1–O6	1.994 (2)	Zn1–O5	1.988 (2)
Cu1–O5	2.204 (2)	Zn1–O6	2.071 (2)
Angles (°)			
N3–Cu1–O4	90.81 (7)	O5–Zn1–N3	112.7 (1)
N3–Cu1–N1	169.81 (7)	O5–Zn1–N1	128.8 (1)
O4–Cu1–N1	81.50 (6)	N3–Zn1–N1	117.97 (9)
N3–Cu1–O6	92.51 (7)	O5–Zn1–O6	88.22 (9)
O4–Cu1–O6	158.00 (9)	N3–Zn1–O6	97.98 (10)
N1–Cu1–O6	92.20 (7)	N1–Zn1–O6	91.96 (8)
N3–Cu1–O5	94.21 (7)	O5–Zn1–O4	87.61 (9)
O4–Cu1–O5	103.90 (7)	N3–Zn1–O4	97.01 (9)
N1–Cu1–O5	94.13 (7)	N1–Zn1–O4	79.44 (8)
O6–Cu1–O5	97.54 (8)	O6–Zn1–O4	164.91 (9)
D–H···A	H···*A* (Å)	*D*···*A* (Å)	*D*–H···*A* (°)
*Complex **3***			
N2–H2···O2^{i}	1.98	2.830 (2)	172
N4–H4···O3^{ii}	2.02	2.870 (3)	169
N4–H4···O4^{ii}	2.61	3.194 (2)	126
O5–H5A···O1^{iii}	1.961 (19)	2.798 (2)	171 (3)
O5–H5B···O2^{iv}	1.965 (18)	2.783 (2)	170 (4)
O6–H6A···O1	1.83 (2)	2.633 (3)	157 (3)
O6–H6B···O3^{v}	1.884 (19)	2.715 (2)	168 (4)
*Complex **4***			
N2–H2···O2^{i}	2.05	2.897 (3)	170
N4–H4···O3^{ii}	1.98	2.822 (3)	166
O6–H6B···O3^{iii}	1.86 (2)	2.680 (3)	179 (4)
O5–H5B···O1^{iv}	1.89 (2)	2.686 (3)	165 (5)
O5–H5A···O2^{v}	1.89 (2)	2.706 (3)	175 (5)
O6–H6A···O1	1.83 (2)	2.634 (3)	162 (4)

Symmetry codes: (i) $x, -y+1/2, z+1/2$; (ii) $-x+1, y-1/2, -z+3/2$; (iii) $-x+1, -y+1, -z+1$; (iv) $x-1, -y+1/2, z-1/2$; (v) $x, -y+1/2, z-1/2$; (vi) $x-1, y, z$ for **3** and (i) $-x+2, -y, -z+1$; (ii) $-x, -y+1, -z$; (iii) $-x+1, -y+1, -z+1$; (iv) $-x+1, -y, -z+1$; (v) $x, y+1, z$ for **4**.

to eight membered rings that can be described as $R_2^2(8)$ [54] (Fig. 4). These intermolecular hydrogen bonding interactions are very important in the construction of the crystal edifice of complexes **3** and **4**. Similar orotate complexes containing double hydrogen bonding interactions were reported [41–45]. In addition, the layers are interlinked together into a network by π···π interactions between both pyrimidine rings of orotate ligand [Cg*A* = N(1)–C(1)–N(2)–C(2)–C(3)–C(4)] (CgA···CgA^{i}) is 3.863 Å for **3** (i = $1-x$, $1-y$, z) and 4.011 Å for **4** (i = $1-x$, $-y$, $1-z$) and imidazole rings [Cg*B* = N(3)–C(6)–C(7)–N(4)–C(8)], the contact distance of two adjacent aromatic rings (CgB···CgB^{i}) is 3.763 for 3 ($-x$, $2-y$, $-z$) and 3.895 Å for **4** (i = $-x$, $2-y$, $-z$). All of these intermolecular interactions give three-dimensional framework results (Fig. 5).

3.3. Antimicrobial activities

The complexes were tested for their in vitro antimicrobial activities against two Gram-positive bacteria (*S. aureus* and *B. cereus*), two Gram-negative bacteria (*E. coli* and *P. aeruginosa*), one fungi *C. albicans* and two clinical isolate (MRSA and *P. aeruginosa*). For

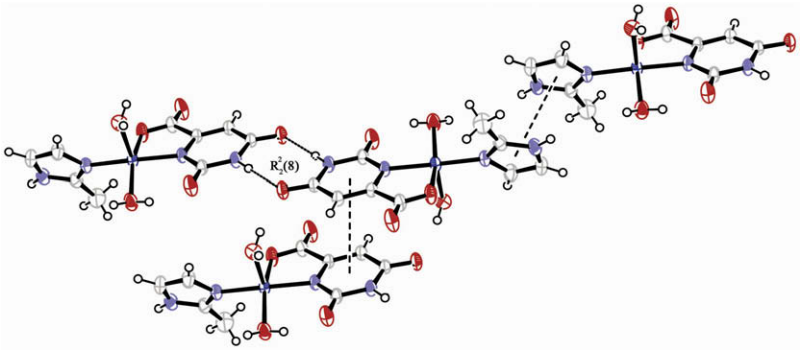

Fig. 4. The π···π and hydrogen bonding interactions of **3** and **4**.

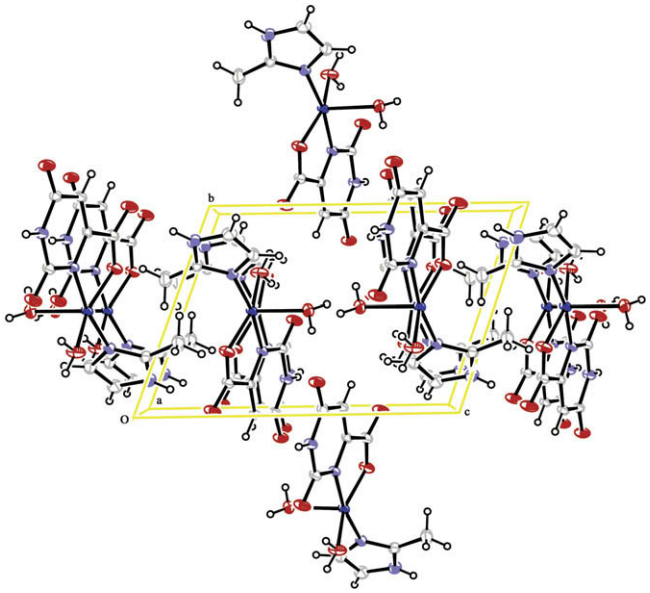

Fig. 5. Packing diagram of **3**.

comparison, the orotic acid and its metal complexes ([Co(HOr)-$(H_2O)_4]\cdot H_2O$ (**5**) [18], $[Ni(HOr)(H_2O)_4]\cdot H_2O$ (**6**) [7], [Cu(HOr)-$(H_2O)_4]\cdot H_2O$ (**7**) [22] and $[Zn(HOr)(H_2O)_4]\cdot H_2O$ (**8**) [7]) were tested for MIC values. The results are presented in Table 5 as minimum inhibitor concentration (MIC) values (μg/mL) which is the minimum concentration to inhibit the growth of bacteria or fungi.

While orotic acid showed activity at higher concentrations on *C. albicans* (2000 μg/mL) and *E. coli* (1375 μg/mL), MICs of other studied microorganism were approximately 1000 μg/mL exception *B. cereus* (750 μg/mL). The antimicrobial activities of **5** and **8** are higher than the orotic acid, **6** and **7** on the all tested microorganisms. While MIC values of **6** according to orotic acid was decreased at *E. coli* (from 1375 to 750 μg/mL), *S. aureus* (from 1000 to 750 μg/mL), *C. albicans* (from 2000 to 750 μg/mL), its activity was increased *P. aeruginosa* (from 1000 to 1500 μg/mL), *B. cereus* (from 750 to 1000 μg/mL), MRSA (from 1000 to 1800 μg/mL) clinical isolate *P. aeruginosa* (from 1000 to 1250 μg/mL). Compared to the orotic acid, the MICs of **7** did not approximately change effective dose on microorganism. Complex **8** had the highest activity on wild type microorganisms between complexes.

The MICs of new complex **1** for strains, gram (−) wild type *E. coli*, *P. aeruginosa*, and clinic isolate *P. aeruginosa* were 800, 700 and 1000 μg/mL respectively, while the growth of *S. aureus*, *B. cereus* and clinic strain MRSA were inhibited more effectively at 400, 400, 250 μg/mL. For **2**, the growth of all the strains with exception MRSA were inhibited at approximately concentration of 1100–1300 μg/mL of the complex, while the MICs for MRSA was 900 μg/mL. **3** had much the same MIC values for all the strains. As can clearly be seen from Table 5, the effective dose of **1**–**4** were, almost without exception, superior to that of metal orotic acid ligands **5**–**8** across all of the bacterial and the fungal strains studied, except for **4** at *S. aureus* and MRSA. As a result, antimicrobial activities were decreased with to be synthesized from **5**–**8** ligands to **1**–**4**. Complex **4** is more effective at both wild type and clinic strain *S. aureus* in comparison to **8** and orotic acids.

1, **4** and **5** have higher activity against Gram-positive than Gram-negative bacteria. In classifying the antibacterial activity as Gram-positive or Gram-negative, it would generally be expected that to be more active against Gram-positive than Gram-negative bacteria because of outer membrane [55]. The **8** has activity on both Gram-positive and Gram-negative bacteria at wild type. The

Table 5
Minimal inhibitory concentration (MIC) values of the complexes against wild type microorganisms (μg/mL) and clinical isolates.

Complexes	Wild type				Clinical isolate		Wild type
	Gram (−)		Gram (+)		Gram(+)	Gram (−)	Eucaryota
	E. coli	*P. aeruginosa*	*S. aureus*	*B. cereus*	Methicillin resistant *S. aureus*	*P. aeruginosa*	*C. albicans*
H_3Or	1375	1000	1000	750	1000	1000	2000
1	800	700	400	400	250	1000	1100
2	1200	1300	1100	1000	900	1100	1300
3	1800	1500	1800	1500	1500	1600	1800
4	800	1500	100	500	100	1300	1500
5	500	500	125	250	125	500	250
6	750	1500	750	1000	1800	1250	1000
7	1000	1000	1500	1000	1375	1250	1000
8	125	250	250	250	500	750	750

Table 6
Antimicrobial assays of same antibiotics against wild type and clinical isolates by disc diffusion method (diameter in mm).

Wild type strains	C (30 μg)	OFX (5 μg)	RD (2 μg)	CXM (30 μg)	TE (30 μg)	N (10 μg)
S. aureus	20	27	27	16	30	–
B. cereus	23	24	9	–	28	–
E. coli	28	30	9	23	27	–
P. aeruginosa	21	17	18	17	20	–
C. albicans	–	–	–	–	–	24
Clinic isolates						
MRSA	22	–	–	–	13	–
P. aeroginosa	–	21	–	–	18	–

C: chloramphenicol, OFX: oflaxacin, RD: rifampicin, CXM: cefuroxime, TE: tetracycline, N: nystatin.

presence of metal ions plays an important role at antimicrobial activity. We think that the disparity at antimicrobial activities between complexes on the microorganisms is change bond characteristics on target area of metal ions because of identical molecular structures of **1**–**8**. Orotic acid and metal complexes have been demonstrated to possess antibacterial and antifungal properties [43,56].

The results of our study indicate that clinic isolates are more resistant than wild type microorganism at standard antibiotics (Table 6). It is a well-known fact that hospital infections are quite important for the public healthy and quite resistant against standard antibiotics. Therefore, there is an urgent demand for new antibiotics and new classes of chemical formula that will efficiently inhibit the growth of pathogenic microorganism. In this study, as part of our efforts into the development of new metal based antimicrobial complexes, new complex **4** could be a new candidate for therapy of *S. aureus* infections and **5** could be candidate for therapy of candidal infection diseases.

Acknowledgment

This work was supported by the Eskişehir Osmangazi University by Project No. 200819042.

Appendix A. Supplementary data

Supplementary data associated with this article can be found, in the online version, at doi:10.1016/j.poly.2009.06.052.

References

[1] C. Janiak, Dalton Trans. (2003) 278.
[2] C.N.R. Rao, S. Natarajan, R. Vaidhyanathan, Angew. Chem., Int. Ed. 43 (2004) 1466.
[3] L. Jiang, X. Feng, C. Su, X. Chen, T. Lu, Inorg. Chem. 46 (2007) 2637.
[4] S.L. James, D.M.P. Mingos, X. Xu, A.J.P. White, D.J. Williams, J. Chem. Soc., Dalton Trans. (1998) 1335.
[5] O.Z. Yeşilel, O. Büyükgüngör, Solid State Sci. 9 (2007) 485.
[6] D. Szeleny, J. Sos, Arzneim.– Forsch. 21 (1991) 777.
[7] M. Sabat, D. Zglinska, B. Jezowska-Trzebiatowska, Acta Crystallogr., Sect. B 36 (1980) 1187.
[8] A. Karipides, B. Thomas, Acta Crystallogr., Sect. C 42 (1986) 1705.
[9] T. Solin, K. Matsumoto, K. Fuwa, Bull. Chem. Soc. Jpn. 54 (1984) 3731.
[10] P. Castan, E. Colacio-Rodriguez, A.L. Beauchamp, S. Cros, S. Wimmer, J. Inorg. Biochem. 38 (1990) 225.
[11] J. Leberman, A. Kornberg, E.S. Simms, J. Biol. Chem. 215 (1955) 403.
[12] P. Castan, E. Colacio-Rodriguez, A.L. Beauchamp, S. Cros, S. Wimmer, J. Inorg. Chem. 38 (1990) 225.
[13] A.Q. Wu, F.K. Zheng, X. Liu, G.C. Guo, L.Z. Cai, Z.C. Dong, Y. Takano, J.S. Huang, Inorg. Chem. Commun. 9 (2006) 347.
[14] C.P. Raptopoulou, V. Tangoulis, V. Psycharis, Inorg. Chem. 39 (2000) 4452.
[15] O.Z. Yeşilel, G. Kaştaş, O. Büyükgüngör, Inorg. Chem. Commun. 10 (2007) 936.
[16] O.Z. Yeşilel, H. Erer, A. Mutlu, O. Büyükgüngör, Polyhedron 28 (2009) 150.
[17] M.J. Plater, M.R.J. Foreman, J.M.S. Skakle, R.A. Howie, Inorg. Chim. Acta 332 (2002) 135.
[18] H. Icbudak, H. Ölmez, O.Z. Yesilel, F. Arslan, P. Naumov, G. Jovanovski, A.R. Ibrahim, A. Usman, H.K. Fun, S. Chantrapromma, S.W. Ng, J. Mol. Struct. 657 (2003) 255.
[19] O.Z. Yeşilel, M.S. Soylu, H. Ölmez, O. Büyükgüngör, Polyhedron 25 (2006) 2985.
[20] O.Z. Yeşilel, H. Ölmez, C. Arıcı, Polyhedron 26 (2007) 3669.
[21] A. Karipides, B. Thomas, Acta Crystallogr., Sect. C 42 (1986) 1705.
[22] D. Michalska, K. Hernik, R. Wysokiński, B. Morzyk-Ociepa, A. Pietraszko, Polyhedron 26 (2007) 4303.
[23] D. Sun, R. Cao, Y. Liang, M. Hong, Y. Zhao, J. Weng, Aust. J. Chem. 55 (2002) 681.
[24] S. Bekiroglu, O. Kristiansson, J. Chem. Soc., Dalton Trans. (2002) 1330.
[25] D.A. Köse, B. Zümreoglu-Karan, O. Şahin, O. Büyükgüngör, J. Mol. Struct. 789 (2006) 147.
[26] D. Mentzafos, N. Katsaros, A. Terzis, Acta Crystallogr., Sect. C 43 (1987) 1905.
[27] X. Li, Q. Shi, D. Sun, W. Bi, R. Cao, Eur. J. Inorg. Chem. (2004) 2747.
[28] I. Mutikainen, Finn. Chem. Lett. (1985) 193.
[29] T.T.B. Ha, A.M. Larsonneur-Galibert, P. Castan, J. Jaud, J. Chem. Crystallogr. 29 (1999) 565.
[30] M.S. Soylu, O.Z. Yeşilel, B. Karabulut, O. Büyükgüngör, Polyhedron 28 (2009) 2487.
[31] O.Z. Yeşilel, F. Tezcan, H. Ölmez, H. Paşaoğlu, O. Büyükgüngör, Z. Anorg. Allg. Chem. 631 (2005) 2497.
[32] A. Bulut, H. İçbudak, O.Z. Yeşilel, H. Ölmez, O. Büyükgüngör, Acta Crystallogr., Sect. E 59 (2003) m736.
[33] O.Z. Yeşilel, H. Olmez, C. Arıcı, Acta Crystallogr., Sect. C 63 (2007) m240.
[34] O.Z. Yeşilel, H. Paşaoğlu, K. Akdağ, O. Büyükgüngör, Z. Anorg. Allg. Chem 633 (2007) 1731.
[35] O.Z. Yeşilel, H. Ölmez, I. Uçar, A. Bulut, C. Kazak, Z. Anorg. Allg. Chem. 631 (2005) 3100.
[36] O.Z. Yeşilel, K. Akdağ, H. Paşaoğlu, O. Büyükgüngör, Z. Naturforsch. 62b (2007) 818.
[37] I. Ucar, A. Bulut, O.Z. Yesilel, H. Ölmez, O. Büyükgüngör, Acta Crystallogr., Sect. C 60 (2004) m563.
[38] O.Z. Yeşilel, E. Şahin, Z. Anorg. Allg. Chem. 633 (2007) 1087.
[39] O.Z. Yeşilel, A. Mutlu, C. Öğretir, O. Büyükgüngör, J. Mol. Struct. 889 (2008) 421.
[40] H. Ölmez, H. İçbudak, O.Z. Yeşilel, C. Arıcı, D. Ülkü, Z. Kristollg. 219 (2004) 300.
[41] O.Z. Yeşilel, H. Paşaoğlu, K. Akdağ, O. Büyükgüngör, Polyhedron 26 (2007) 2761.
[42] O.Z. Yeşilel, H. Ölmez, H. Içbudak, O. Büyükgüngör, Z. Naturforsch. 60b (2005) 1138.
[43] O.Z. Yeşilel, N. Dege, C. Darcan, O. Büyükgüngör, Z. Naturforsch. 62b (2007) 1590.
[44] O.Z. Yeşilel, I. Uçar, A. Bulut, H. Ölmez, O. Büyükgüngör, Z. Naturforsch. 61b (2006) 147.
[45] O.Z. Yeşilel, H. Paşaoğlu, K. Akdağ, O. Büyükgüngör, Z. Anorg. Allg. Chem. 633 (2007) 1731.
[46] Stoe & Cie, X-AREA (Version 1.18), X-RED32 (Version 1.04), Stoe & Cie, Darmstadt, Germany, 2002.
[47] A. Altomare, M.C. Burla, M. Camalli, G.L. Cascarano, C. Giacovazzo, A. Guagliardi, A.G.G. Moliterni, G. Polidori, R. Spagna, J. Appl. Crystallogr. 32 (1999) 115.
[48] G.M. Sheldrick, SHELXS97, University of Göttingen, Germany, 1997.
[49] L.J. Farrugia, J. Appl. Crystallogr. 30 (1997) 565.
[50] Clinical and Laboratory Standards Institute, Methods for dilution antimicrobial susceptibility tests for bacteria that grow aerobically; approved standard, 7th ed. CLSI document M7–A7. Clinical Laboratory Standards Institute, Wayne, PA, 2006.
[51] O.Z. Yeşilel, H. Ölmez, H. İçbudak, J. Therm. Anal. Calorim. 89 (2007) 555.
[52] A. Hernanz, F. Billes, I. Bratu, R. Navarro, Biopolymers 57 (2000) 187.
[53] L. Xing, C. Rong, S.D. Fong, H.M. Chun, Chinese J. Struct. Chem. 21 (2002) 374.
[54] M.C. Etter, J.C. MacDonald, J. Bernstein, Acta Crystallogr., Sect. B 46 (1990) 256.
[55] A.R. Mc Cutcheon, S.M. Ellis, R.E.W. Hancock, G.H.N. Towers, J. Ethnopharmacol. 37 (1992) 213.
[56] P. Ruasmadiedo, J.C. Badagancedo, E.G. Fernandez, D.G. Dellano, C.G. Delos Reyes Gavilan, J. Food Protect. 59 (1996) 502.